AGU PUBLICATIONS

JGR

Journal of Geophysical Research: Biogeosciences

RESEARCH ARTICLE
10.1002/2016JG003622

Key Points:
- Disturbances in the western United States impact LST and GPP with varying results among ecoregions and disturbance types
- In general, disturbance results in increased LST and decreased GPP
- Biophysical disturbance responses are driven by severity and interannual changes in air temperature

Supporting Information:
- Supporting Information S1

Correspondence to:
L. A. Cooper,
leila.cooper@umconnect.edu

Citation:
Cooper, L. A., A. P. Ballantyne, Z. A. Holden, and E. L. Landguth (2017), Disturbance impacts on land surface temperature and gross primary productivity in the western United States, *J. Geophys. Res. Biogeosci.*, *122*, 930–946, doi:10.1002/2016JG003622.

Received 9 SEP 2016
Accepted 22 MAR 2017
Accepted article online 31 MAR 2017
Published online 27 APR 2017

Disturbance impacts on land surface temperature and gross primary productivity in the western United States

L. Annie Cooper[1], Ashley P. Ballantyne[1], Zachary A. Holden[2], and Erin L. Landguth[3]

[1]Department of Ecosystem and Conservation Sciences, University of Montana, Missoula, Montana, USA, [2]U.S. Forest Service, Missoula, Montana, USA, [3]Division of Biological Sciences, University of Montana, Missoula, Montana, USA

Abstract Forest disturbances influence forest structure, composition, and function and may impact climate through changes in net radiation or through shifts in carbon exchange. Climate impacts vary depending on environmental variables and disturbance characteristics, yet few studies have investigated disturbance impacts over large, environmentally heterogeneous, regions. We used satellite data to objectively determine the impacts of fire, bark beetles, defoliators, and "unidentified disturbances" (UDs) on land surface temperature (LST) and gross primary productivity (GPP) across the western United States (U.S.). We investigated immediate disturbance impacts, the drivers of those impacts, and long-term postdisturbance LST and GPP recovery patterns. All disturbance types caused LST increases (°C; fire: 3.45 ± 3.02, bark beetles: 0.76 ± 3.04, defoliators: 0.49 ± 3.12, and UD: 0.76 ± 3.03). Fire and insects resulted in GPP declines (%; fire: −25.05 ± 21.67, bark beetles: −2.84 ± 21.06, defoliators: −0.23 ± 15.40), while UDs resulted in slightly enhanced GPP (1.89 ± 24.20%). Disturbance responses also varied between ecoregions. Severity and interannual changes in air temperature were the primary drivers of short-term disturbance responses, and severity also had a strong impact on long-term recovery patterns. These results suggest a potential climate feedback due to disturbance-induced biophysical changes that may strengthen as disturbance regimes shift due to climate change.

1. Introduction

Forests cover roughly 30% of Earth's land surface and provide vital ecosystem services, such as water quality, wildlife habitat, and timber production, as well as climate services [*Bonan*, 2008]. The ability of forests to continue providing these ecosystem services depends on forest characteristics, such as stand structure, composition, and functional processes. The primary drivers of forest characteristics are state factors including climate, soils, and topography. However, secondary drivers, such as disturbance (e.g., wildfire, insect attack, or windthrow), are often more important than state factors in determining ecosystem services at the regional scale [*Law et al.*, 2003; *Pregitzer and Euskirchen*, 2004; *Bond-Lamberty et al.*, 2007], influencing stand composition and stand age, as well as C fluxes, nutrient cycling, and energy dynamics. As such, disturbance is an integral process in all forest ecosystems and altered disturbance regimes have the potential to impact forest health globally.

Although disturbance agents such as insect outbreaks and stand-replacing wildfires play a major role in shaping forest ecosystems, global change may be altering disturbance regimes in the United States (U.S.) and elsewhere. Disturbance events affect large swathes of forest in North America every year, with wildfires affecting approximately 760,000 ha/yr [*Littell et al.*, 2009] and insect-induced mortality affecting approximately 100,000 to 1,000,000 ha/yr [*Hicke et al.*, 2012; *Meddens et al.*, 2012]. While disturbance regimes vary in frequency and severity, more severe disturbance events, such as stand-replacing wildfires and severe bark beetle outbreaks, may be increasing in frequency as global temperatures rise [*Watson et al.*, 1998; *Adams et al.*, 2009; *Bentz et al.*, 2010; *Westerling et al.*, 2011; *Hicke et al.*, 2012; *Millar and Stephenson*, 2015]. The extent and magnitude to which disturbance has altered certain ecosystem services, including climate regulation, is often regionally specific [*Randerson et al.*, 2006].

Disturbance events vary widely in severity and extent, and their ecological impacts are mediated by climate, topography, and predisturbance vegetation characteristics [*Holden et al.*, 2009; *Dillon et al.*, 2011]. These impacts can include everything from decreases in stand-level productivity [*Hanson and Weltzin*, 2000; *Kurz et al.*, 2008] to changes in the radiative budget of the surface [*Randerson et al.*, 2006; *Maness et al.*, 2013]. Many studies have focused on the impacts of disturbance on successional patterns, forest structure, and

composition [e.g., *Sousa*, 1984; *Johnson et al*., 1998]; however, disturbance effects on local and regional climate are less studied. Therefore, understanding how disturbances of varying severity and frequency impact climate is critical for predicting forest resilience and the recovery of vital ecosystem services.

Disturbance can influence climate in several ways, including altering the radiative budget of forests or by affecting the uptake and release of C by forests. *Kurz et al*. [2008] estimated that large forested regions of British Columbia (BC), Canada, switched from a C sink to a C source following a large and severe mountain pine beetle (MPB) outbreak. The conversion in net C flux was expected to occur over several decades, suggesting that severe biotic disturbances have gradual, but long-term, impacts. These modeled results were supported by an observed 15–20% decline in satellite-derived GPP immediately postoutbreak [*Coops and Wulder*, 2010]. Although increased albedo following beetle outbreaks in both BC and the western U.S. results in a decline in absorbed radiation [*O'Halloran et al*., 2012; *Maness et al*., 2013; *Vanderhoof et al*., 2013], a decrease in summertime evapotranspiration (ET) results in an increase in the sensible to latent heat ratio (i.e., Bowen ratio). These effects combined to ultimately result in an ~1°C increase in surface temperature following the BC outbreak [*Maness et al*., 2013].

Despite the relatively consistent findings regarding post-MPB outbreak C fluxes, these studies focused on an area with a very large and severe insect outbreak; results may differ when outbreaks occur on smaller scales or under different environmental conditions. For example, the effects of less severe disturbance and mortality events, such as smaller-scale insect outbreaks and drought, are more ambiguous than the results from the MPB outbreak in BC. *Hanson and Weltzin* [2000] determined that the likely effects of drought are reductions in net primary production and stand water use, both phenomena resulting in positive radiative forcing (i.e., an atmospheric warming effect). However, changes in albedo or heterotrophic respiration were not included in the analysis, making it difficult to assess the net radiative forcing resulting from smaller and less severe disturbances such as drought. Thus, the exact climate effects of these disturbances are unclear and likely depend on the extent and severity of the event as well as the environmental characteristics of the forest ecosystem (e.g., vegetation type).

Wildfire also appears to have a large effect on the net radiative forcing of ecosystems [*Randerson et al*., 2006], although the effect is not well understood across different forest ecosystems. Fires in boreal Alaska were found to have differing impacts on climate depending on the time since disturbance [*Randerson et al*., 2006]. Initially, observations showed that fires resulted in positive radiative forcing due to large C emissions and the deposition of black C on ice and snow, decreasing the albedo of the surface and increasing absorbed radiation. However, according to model simulations, after several decades, boreal forest fires resulted in a net negative radiative forcing due to increases in surface albedo as a result of decreased canopy cover, ultimately leading to a potential cooling of the land surface. This is one of the few studies to develop a physical framework to evaluate the net radiative impacts of the effects of forest disturbance, but it only addressed a relatively small forested site and a single fire event.

Another study [*O'Halloran et al*., 2012] addressed the radiative impacts of fire, bark beetle attack, and hurricanes due to changes in albedo and the net ecosystem carbon balance over several locations across North America. The authors found results similar to those of *Randerson et al*. [2006] for boreal wildfire, with an initial warming effect, followed several decades later by a slight cooling effect. However, they found that bark beetle attack increased wintertime albedo, resulting in negative radiative forcing. This complicates the longer-term results of *Kurz et al*. [2008], which suggest positive radiative forcing from bark beetle attack over many decades. These results demonstrate differences in climate impacts among disturbances and disturbance locations and highlight the need for systematic analyses across larger areas.

Several other studies have addressed the potential for disturbances to impact climate in temperate regions through both biogeochemical [*Hanson and Weltzin*, 2000; *Kurz et al*., 2008; *Hicke et al*., 2012; *Seidl et al*., 2014] and biogeophysical [*Vanderhoof et al*., 2013; *Maness et al*., 2013] effects, with results indicating that temperate disturbances may generally result in a long-term net positive radiative forcing, although the forcing depends on disturbance location, timing, type, and severity. The continued complexity of disturbance-related climate forcing in forest ecosystems indicates that an analysis evaluating the patterns of effects of multiple disturbance types on local to regional climate across multiple ecosystems is a novel contribution to the field. There is a general consensus that forests will become more vulnerable to disturbance as a result of increasing water and heat stress [*Allen et al*., 2010; *Heyder et al*., 2011; *Anderegg et al*., 2013], but in order to better

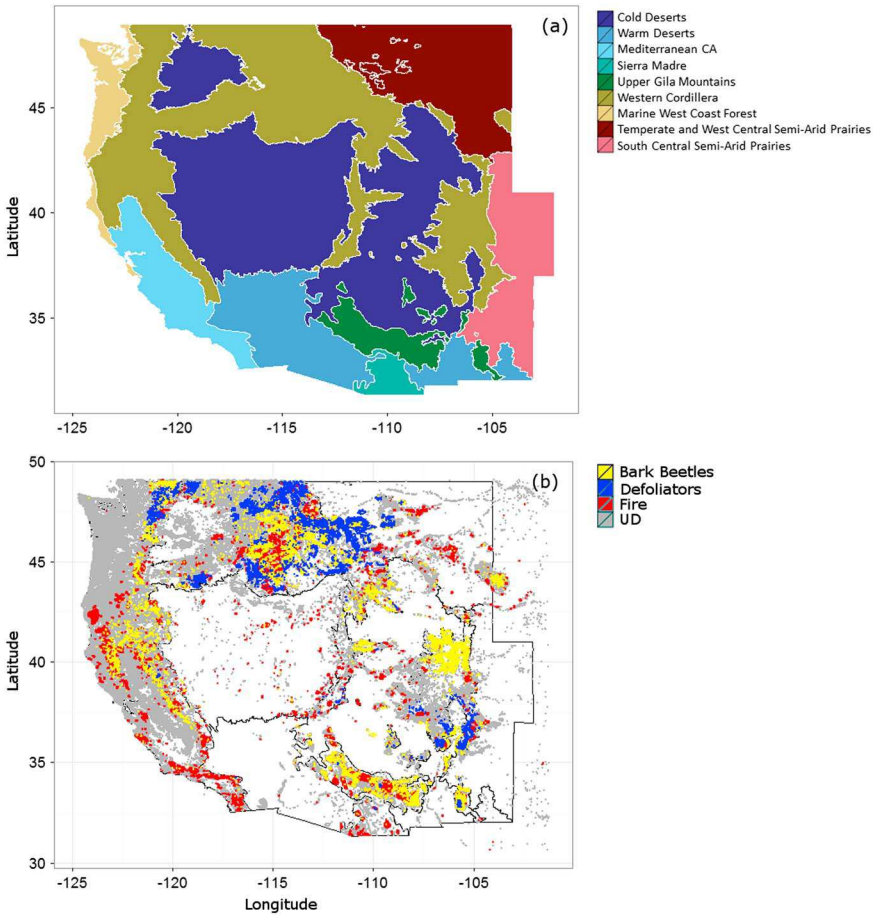

Figure 1. (a) Map of ecoregions used in the study. Ecoregions were limited to 11 states (WA, OR, CA, ID, NV, AZ, MT, UT, WY, CO, and NM). (b) Location of disturbances across the western U.S. Note that disturbances shown *are not* to size, and actual pixel size is smaller than map representation.

manage for forest resilience to climate change, it is also necessary to understand the effects of forest disturbances on local- to regional-scale climate.

The aim of this study is to determine the impact of fires, bark beetles, defoliators, and "unidentified disturbances" (UDs) on land surface temperature (LST) and gross primary productivity (GPP) in the western U.S. from 2002 to 2012. Specifically, our analysis seeks to answer the following research questions: (1) How do LST and GPP change immediately following disturbance in forests of the western U.S.? (2) How do these short-term effects differ among ecoregions and disturbance types? (3) How important are severity, extent, and interannual air temperature change to the short-term disturbance response of LST and GPP? And (4) how do LST and GPP change over 12 years following disturbance? This study adds to the literature through an analysis of disturbance effects across ecoregions and four disturbance categories. It covers a large geographical region and provides a summary of the relative importance of disturbances of varying types and locations on local- to regional-scale climate.

2. Methods

2.1. Study Area

We assessed the impacts of disturbance over the western U.S. (Figure 1a), a region encompassing substantial topographic and climatic variation. Mean annual temperatures range from −3°C in the Intermountain west to 24°C in the southwest [*PRISM Climate Group*, 2011], and mean annual precipitation ranges from 5925 mm in the Pacific northwest to 62 mm in the desert southwest [*PRISM Climate Group*, 2011].

A range of disturbances are known to impact western forests, including prescribed and wildland fires, insects and pathogens, windthrow, and timber harvest. Substantial efforts to map wildfires and insect-induced mortality have resulted in spatially explicit annual maps of these disturbance types. We therefore focus primarily on these disturbance types and classify all other forms of disturbance as UD. Furthermore, as our disturbance detection approach was limited to detecting only disturbances affecting moderately large areas of the landscape, insect species included in the insect damage categories were limited to species of aggressive bark beetles and defoliators [see *Hicke et al*., 2012]. Bark beetle species included mountain pine beetle (*Dendroctonus ponderosae*), western pine beetle (*Dendroctonus brevicomis*), and species of ips (*Ips sp*.). Defoliators included western spruce budworm (*Choristoneura occidentalis*), western black-headed budworm (*Acleris gloverana*), western hemlock looper (*Lambdina fiscellaris spp. lugubrosa*), pine needlesheath miner (*Zelleria haimbachi*), sawflies (Suborder *Symphyta*), tent caterpillars (*Malacosoma sp*.), and Douglas fir tussock moth (*Orygia pseudostugata*).

2.2. Disturbance Detection and Grouping by Disturbance and Ecoregion

Disturbances were mapped using a combination of satellite imagery and aerial data sources, including Moderate Resolution Imaging Spectroradiometer (MODIS) Enhanced Vegetation Index (EVI) time series imagery (http://lpdaac.usgs.gov), Monitoring Trends in Burn Severity (MTBS) data [*Eidenshink et al*., 2007], and Aerial Detection Survey (ADS) maps (USDA Forest Service, Forest Health Protection and its partners). EVI time series data for 2000–2014 were accessed between July and September 2014. These data are available at 250 m resolution and are collected via the Terra satellite every 16 days. EVI was used rather than the Normalized Difference Vegetation Index (NDVI) because it is less susceptible to saturation in dense canopies [*Liu and Huete*, 1995]. The index is calculated as

$$\mathrm{EVI} = G \times \frac{(\rho_{\mathrm{nir}} - \rho_{\mathrm{red}})}{(L + \rho_{\mathrm{nir}} + C_1\rho_{\mathrm{red}} + C_2\rho_{\mathrm{blue}})} \quad (1)$$

where G is the gain factor, ρ_{nir} and ρ_{red} are atmospherically corrected surface reflectances, L is the canopy background adjustment term, and C_1 and C_2 are coefficients for the aerosol resistance term [*Huete et al*., 2002]. While the blue band used for correcting residual atmospheric effects ($C_2\rho_{\mathrm{blue}}$) is only available at 500 m rather than 250 m, this should have negligible impacts on results (http://lpdaac.usgs.gov).

Raw EVI images were preprocessed for quality assurance, and pixels determined to be either cloudy or unreliable due to satellite measurement abnormalities were removed. Images were further processed to remove nonforested pixels according to a 20% forest mask created from the 250 m resolution MODIS Vegetation Continuous Fields product [*DiMiceli et al*., 2011; *Townshend et al*., 2011]. Forested images were then mosaicked to cover the western U.S. and run through a preprocessing algorithm to remove outliers and replace missing values by interpolation, using the "interpts" function in the "wq" package [*Jassby and Cloern*, 2015] in R [*R Core Team*, 2013], resulting in spatially and temporally continuous time series of EVI values. Outliers were determined as values lying outside of 150% of the first or third quartiles of the EVI value distribution. Because the time series were evaluated for change at the pixel level, we were further able to selectively remove pixels where (a) more than one quarter of the total measurement days were missing or (b) more than 20 consecutive measurement days were missing.

We then used the Breaks for Additive Season and Trend (BFAST) change detection algorithm [*Verbesselt et al*., 2010a, 2010b] to determine areas of likely disturbance between 2002 and 2012 at the pixel level (i.e., 250 m). The BFAST algorithm decomposes time series into seasonal, trend, and noise components and then compares slopes of trend segments iteratively to find breakpoints [*Verbesselt et al*., 2010a, 2010b]. We used the BFAST algorithm with a harmonic seasonal component and a single allowable breakpoint. With a single breakpoint, only 1 year per pixel could show disturbance, resulting in the pixel disturbance being the largest break in the time series (if breaks were detected) and thus the most severe disturbance in that pixel. BFAST could not detect disturbances 2000–2001 and 2013–2014 due to lead-in requirements within the algorithm. Pixels with significant detected decreases in the EVI time series were labeled with the year of change and compiled into annual raster files.

In an effort to improve the detection of disturbed pixels in cloud- and snow-contaminated areas, we augmented the BFAST results with data on forest loss from *Hansen et al*. [2013]. The Hansen data were originally computed annually at 30 m resolution using Landsat imagery, thus increasing the likelihood of catching a

cloud-free segment of the landscape. For this analysis, these 30 m data were aggregated to 240 m resolution to approximate the resolution of the MODIS data. The coarser-resolution forest loss files were then placed onto a grid equivalent in resolution and extent to the BFAST results grid, with Hansen raster values added to the nearest BFAST-equivalent grid pixels. Once equivalent grids were achieved, the Hansen and BFAST detection rasters were mosaicked to a final disturbance raster, with disturbances marked if they were shown on either of the two detection rasters (Figure 1b). Data from *Hansen et al*. [2013] were prepared and downloaded from Google Earth Engine [see *Hansen et al*., 2013] in August 2015. Raster files were mosaicked in ArcGIS [*Esri*, 2010].

The combined disturbance data were split into four distinct disturbance type categories—(1) fire, (2) bark beetles, (3) defoliators, and (4) UD. Fire disturbance pixels were identified as pixels where the combined disturbance data for a given year overlapped MTBS fire polygons for that same year. Insect disturbance pixels, including bark beetles and defoliators, were determined as pixels where the combined disturbance data for a given year overlapped the ADS polygons labeled as bark beetle or defoliator mortality for any year between 2002 and 2012. Insect damage may only reach an EVI-detectable severity after several years, although the outbreak may be detected in the ADS maps at the very start of the outbreak. Alternatively, ADS data may mark the disturbance after it is detected by satellite methods. Thus, it was assumed that if the pixel was within the bounds of the ADS polygon, it was most likely an insect damage pixel. This assumption was not made for fires because all damage occurs within a single year, allowing for much more accurate identification and timing. Where fire and insect damage polygons overlapped, the pixel was labeled "fire" if the detection year matched the year of the fire and labeled "bark beetle" or "defoliator" if the detection year did not match the year of the fire. The UD category was applied to all other pixels that did not fall under the previous categories.

MTBS and ADS presence or absence values were extracted at disturbance detection points in ArcGIS [*Esri*, 2010] in order to indicate the mode of disturbance for that pixel. ADS polygons were limited to those containing damage attributed to the bark beetle and defoliator species listed in section 2.1. We chose not to use a cutoff for trees killed per acre within ADS polygons, as mortality area is patchy within the affected area polygons, making polygon-level trees killed per acre unrepresentative of all pixels within each polygon.

Lastly, results were evaluated by ecoregions as defined by the Environmental Protection Agency's Level II ecological region product [*Omernik*, 1987; *Omernik and Griffith*, 2014]. Data were grouped into ecoregions according strictly to the Level II regions at first, and then regions with fewer than 50 detected disturbance pixels were combined with the ecoregion nearest to them in both location and vegetation type (Figure 1a).

Detection results were evaluated for accuracy using two methods, (1) evaluation relative to ADS (USDA Forest Service, Forest Health Protection and its partners) and MTBS polygons [*Eidenshink et al*., 2007] and (2) comparison with 2002–2010 detection results from the well-validated Vegetation Change Tracker (VCT) project [*Huang et al*., 2010; *Zhao et al*., 2015]. The first method indicated mixed results for the number of ADS and MTBS polygons that were detected by the combined BFAST and Hansen data set (Table S3 in the supporting information). For example, ADS bark beetle polygons were often undetected, but most MTBS polygons were detected. Those polygons that were not detected by the data set tended to be smaller and had lower recorded severity (Table S3). The second validation method demonstrated similar overlap between VCT-detected pixels and ADS and MTBS polygons as method 1, suggesting general agreement between VCT and the data set used here in detecting disturbance (Table S3). Additionally, an examination of the distances between BFAST/Hansen points and VCT points indicated similarities in areas of detection (Figure S9 and Table S4). The detection areas that did not match were primarily in UD areas.

2.3. Response and Predictor Variable Preparation

Mean summertime (June–July–August; JJA) Landsat-based 30 m LST data were prepared in Google Earth Engine in August 2015 using methods described in *Weng et al*. [2004] and *Sobrino et al*. [2004]. In short, this method for estimating LST uses an estimated land surface emissivity based on NDVI [*Sobrino et al*., 2004] as input into the equation

$$\mathrm{LST} = \frac{T_B}{1 + \left(\lambda \times \frac{T_B}{\rho}\right)} \ln \varepsilon \tag{2}$$

where T_B is the effective at-satellite temperature (K), λ is the wavelength of emitted radiance (μm), ε is NDVI-based emissivity, and $\rho = h \times {}^{c}/_{\sigma}$, with h equal to Planck's constant (J s), c equal to the speed of light (m s^{-1}), and σ equal to the Boltzmann constant (J K^{-1}) [*Weng et al.*, 2004]. The resulting product was aggregated to 240 m to better match the detection data. Landsat data are available from the U.S. Geological Survey.

Changes in GPP were estimated using the 1 km, 8 day, MOD17A2 GPP product. Data were downloaded via the Land Processes Distributed Active Archive Center in September 2015, and pixels flagged as low quality were removed.

Factors (i.e., predictor variables) potentially influencing the disturbance response variables included disturbance severity (S), extent (E), and local interannual change in air temperature (T_{air}). S was determined as the per-pixel change in predisturbance to postdisturbance EVI (see equations (5) and (6)). The E of fire disturbance events was labeled as the total acres burned, retrieved from the MTBS fire polygon data. Each fire pixel was labeled with the total area of the fire. The E of bark beetle, defoliator, and UD events was estimated as the size of the area covered by adjoining pixels detected in the same year. The calculation of area for insect and UD disturbances was done in ArcGIS [*Esri*, 2010]. We chose to label each pixel with the area of the total disturbance (encompassing several pixels), because we were interested in how disturbance in surrounding pixels influences the effects within single pixels. For example, a large fire may cause a larger increase in LST in some pixels because surrounding pixels no longer have surviving vegetation, and thus higher ET, to mitigate that pixel's rising LST.

PRISM monthly 800 m temperature data [*PRISM Climate Group*, 2011] averaged for JJA were used to represent local air temperatures, for use in determining how the disturbance response results were influenced by nondisturbance-related differences in temperature. T_{air} was calculated as the predisturbance to postdisturbance change in the variable (see equations (5) and (6)). Data were downloaded from the PRISM website in October 2015.

It should be noted that the aim of this analysis was not to identify the drivers of fires, bark beetle outbreaks, or defoliator attacks but rather to identify what disturbance or environmental factors have the strongest influences on the responses of LST and GPP following disturbance. Many other studies have identified the drivers of disturbance [e.g., *Raffa et al.*, 2008; *Dillon et al.*, 2011; *Westerling et al.*, 2011].

2.4. Analysis of Disturbance-Related Changes in LST and GPP

The LST difference and GPP percent change following the disturbance were calculated at the pixel level. Only changes in the JJA values of the variable were analyzed for this study. Values for each variable before (V_{pre}) and after (V_{post}) the detected disturbance were calculated as follows:

$$V_{pre} = \frac{(V_{t-1} + V_{t-2})}{2} \tag{3}$$

$$V_{post} = \frac{(V_t + V_{t+1})}{2} \tag{4}$$

where V_t is the variable at t years before or after the detected disturbance. We then calculated the absolute (ΔV) and percent change (% ΔV) in each variable as

$$\Delta V = V_{post} - V_{pre} \tag{5}$$

$$\%\Delta V = \left(\frac{V_{post} - V_{pre}}{V_{pre}}\right) \times 100 \tag{6}$$

All calculations were completed in R [*R Core Team*, 2013].

2.5. Statistical Analyses

After response variables were extracted at each detected disturbance point, differences in disturbance effects between ecoregions and disturbance types were examined. The significance of the differences between both ecoregions and disturbance types was determined using multivariate analysis of variance (MANOVA) tests. If significant differences in disturbance response variables (LST and GPP) were found, discriminant function

Table 1. Variables Included in the Random Forest Models[a]

Predictor Variable	Abbreviation	Reasoning
Severity (% decline in EVI)	S	A higher degree of mortality (i.e., higher severity) in the pixel will separate it from the original state more than a lower degree of mortality.
Local interannual change in air temperature	T_{air}	A change in the average JJA air T will influence soil moisture and therefore latent heat exchange, surface temperatures, and photosynthesis (GPP).
Extent	E	Disturbances that cover the entire pixel should have a larger impact on the response variables than small (<1 pixel) disturbance patches. Responses to smaller disturbances may be diluted by undisturbed patches of forest.
Disturbance type	D	Included for comparison with the above variables. Disturbance type should have a strong influence on the average LST, GPP, and C stock response because each disturbance type affects forest structure and composition differently.
Ecoregion	R	Also included for comparison with S, T_{air}, and E_a. Environmental characteristics, including soils, vegetation, climate, and hydrology, differ by ecoregion and may impact disturbance responses.

[a] S, T_{air}, and E_a are continuous variables. D and R are factors.

analysis was conducted to determine the ability of the response variables to predict the type of disturbance that caused the response and the ecoregion in which the disturbance occurred. MANOVA tests were conducted in R [*R Core Team*, 2013]. Discriminant function analysis was also done in R using the "lda" function in the "MASS" package [*Venables and Ripley*, 2002].

To analyze the influence of the potential drivers of disturbance impacts, regression trees were created using the "randomForest" function within the randomForest package [*Liaw and Wiener*, 2002] in R. One model was created for each response variable (i.e., LST and GPP), resulting in two total models. The importance S, E, and T_{air} to the response variables was identified by mean squared error (MSE) importance values from the random forest models. Ecoregion and disturbance type were also included in the models as potential driving factors (Table 1).

To determine how the disturbance responses of LST and GPP change through time, data were collected for all years following disturbance events through 2014. Predisturbance to postdisturbance changes in LST and GPP were used to identify the patterns in recovery following disturbances segregated by four severity classes (0–20%, 21–40%, 41–60%, and >60%), with percent decline in EVI used as a proxy for severity (Figure S10). Recovery data were prepared with the same methods used to calculate initial disturbance response (equations (5) and (6)), with V_{post} representing only 1 year rather than the average of 2 years. Line graphs of recovery were analyzed by time to stabilization and compared by disturbance type, ecoregion, and severity category. The time period of the analysis (2002–2012) was insufficient to see full recovery following disturbance. However, "stabilization," or leveling in the response variables following the disturbance, may result due to other factors, including regrowth of noncanopy vegetation. This stabilization, if seen, indicated some degree of recovery and is used here as an indication of future trends in recovery.

3. Results

3.1. Changes in LST and GPP in Response to Disturbance

3.1.1. Fire

We observed a significant increase in LST and a decline in GPP following fire events (Figure 2 and Table S2). The mean LST increase (°C) was 3.45 ± 3.02 ($\mu \pm \sigma$) over all regions (Figure 2a), although there was considerable interregional variation (Figure 3). Cold Deserts experienced the largest increases in LST (4.57 ± 3.45), while the Marine West Coast Forests experienced the smallest increases (1.10 ± 1.98). Fires also resulted in significant declines in GPP (Figure 2b). Across all regions, the mean GPP percent change was −25.05 ± 21.67. The fire effect on GPP varied significantly by ecoregion (Figure 3). The largest declines in GPP were seen in the Warm Deserts (−41.49 ± 23.81), and the smallest declines were observed in Marine West Coast Forests (−4.72 ± 11.38).

3.1.2. Bark Beetles

Following bark beetle outbreaks, LST generally increased, and response of GPP was variable across ecoregions (Figure 2 and Table S2). All but two regions, the Sierra Madre and Temperate/West Central

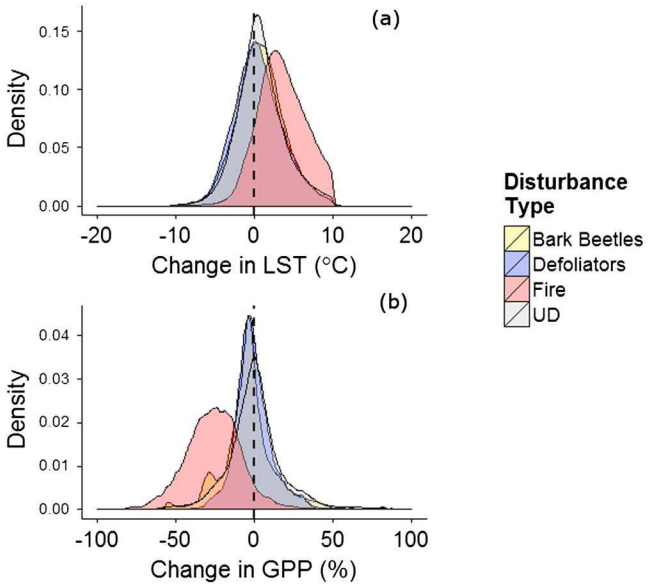

Figure 2. Density distributions of JJA changes in (a) LST and (b) GPP following fire, bark beetle attack, defoliator attack, and UDs.

Semi-Arid Prairies, showed increases in LST following bark beetle outbreaks (Figure 2a). The mean impact of bark beetles on LST (°C) was 0.76 ± 3.04. The largest increase in LST was seen in the Western Cordillera (0.92 ± 3.00), and the smallest increase was seen in Warm Deserts (0.01 ± 0.87). Bark beetle disturbance occurring in Sierra Madre and Temperate/West Central Semi-Arid Prairies resulted in slight decreases in LST (−0.05 ± 3.13 and −0.18 ± 2.89). The mean impact of bark beetle outbreaks was a percent change in GPP of −2.84 ± 21.06, although seven of the nine ecoregions showed a slight increase in GPP (Figure 3). The greatest increase in GPP occurred in Warm Deserts (29.86 ± 37.09), although there were also increases in the Cold Deserts, Sierra Madre, Upper Gila Mountains, Marine West Coast Forests, and all Semi-Arid Prairies. GPP decreased postdisturbance in Mediterranean California and the Western Cordillera (−1.02 ± 17.01 and −4.43 ± 13.80).

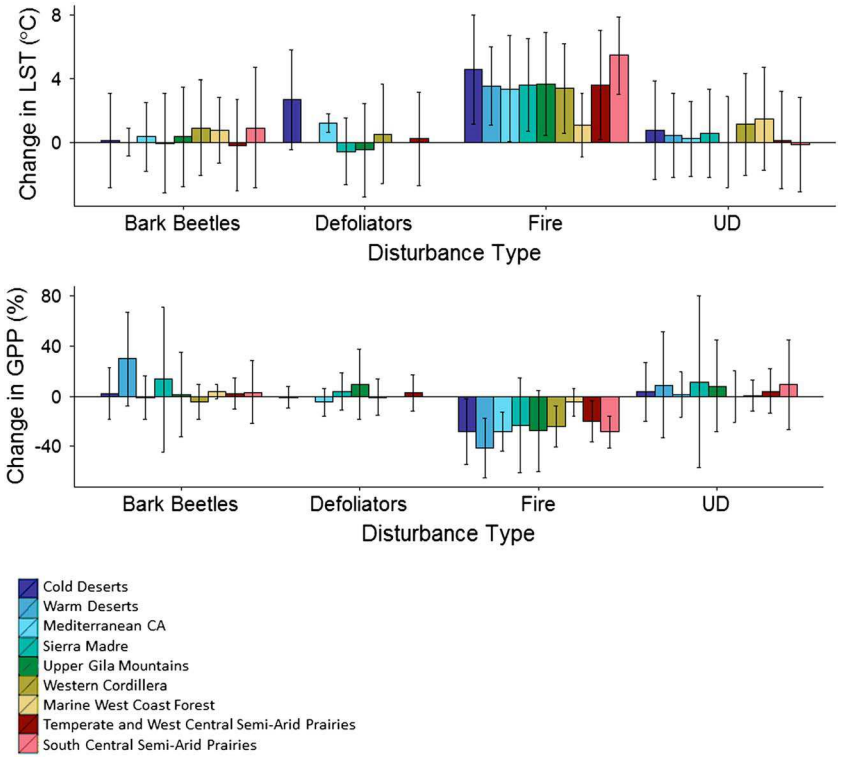

Figure 3. JJA change in response variables by ecoregion. Bar height is the mean response for the ecoregion; error bars represent standard deviation.

3.1.3. Defoliators

Overall, LST increased slightly and GPP decreased slightly following defoliator attacks (Figure 2 and Table S2). The average LST effect over all regions was 0.49 ± 3.12°C, with four ecoregions showing increases in LST and two ecoregions showing decreases. An additional three ecoregions had no data. The largest increases in LST following defoliator attack occurred in Cold Deserts (2.68 ± 3.00). The Sierra Madre and Upper Gila Mountain ecoregions showed decreases in LST (−0.56 ± 2.12 and −0.48 ± 2.94). The overall defoliator effect on GPP (%) was very small (−0.23 ± 15.40), with substantial variation between ecoregions. The Upper Gila Mountain ecoregion showed large increases in GPP following defoliator attacks (9.68 ± 27.91), while Mediterranean CA showed moderate GPP declines (−4.51 ± 10.97).

3.1.4. Unidentified Disturbance

In general, LST and GPP increased following UDs (Figure 2 and Table S2). The mean LST effect (0.76 ± 3.03°C) and regional variability were very similar to the patterns following insect outbreaks (Figure 2). The ecoregion with the largest increase in LST was the Marine West Coast Forest ecoregion (1.48 ± 3.24). LST decreased in the South Central Semi-Arid Prairies following UDs (−0.15 ± 2.97). GPP generally increased following UDs, with variation in response between ecoregions (Figure 3). The mean percent change in GPP was 1.89 ± 24.20. The largest increases in GPP occurred in four regions: Warm Deserts (9.13 ± 42.16), Sierra Madre (11.48 ± 68.57), Upper Gila Mountains (8.03 ± 36.55), and South Central Semi-Arid Prairies (9.26 ± 34.99). The Western Cordillera showed a slight decrease in GPP (−0.35 ± 20.28).

3.2. Differences in Disturbance Response Between Disturbance Types and Ecoregions

MANOVA tests indicated that there were highly significant differences in LST and GPP responses due to disturbance type ($F(6, 4883470) = 59{,}477$, $p < 0.01$), ecoregion ($F(16, 4883470) = 4735$, $p < 0.01$), and the interactive effect of disturbance type and ecoregion ($F(42, 4883470) = 516$, $p < 0.01$). In order to ensure that the large sample size was not confounding the significance of the results, MANOVA tests were also conducted on 2000 samples of 1000 detected disturbance points and the statistics of each of those 2000 samples averaged to determine the significance of lower sample size on the factor differences. Disturbance ($F(6, 1960) = 25.98$, $p < 0.01$) and ecoregion ($F(16, 1960) = 3.47$, $p < 0.01$) remained significant, despite the lower sample size. The interactive effect between disturbance type and ecoregion became insignificant ($F(17, 1960) = 1.66$, $p = 0.20$).

Discriminate function analysis was used to determine whether the responses of LST and GPP were sufficiently different to classify detected pixels into disturbance types and ecoregions. A linear model using the response variables (LST and GPP) as predictor variables predicted disturbance type with 83.98% accuracy. The response variables resulted in lower accuracy when predicting ecoregion (49.76% accuracy). However, when the data were subset by disturbance type, linear models predicted ecoregion with higher accuracy for bark beetle attack (72.92%) and defoliator damage (92.95% accuracy) than for fire (57.25% accuracy) and UDs (46.36% accuracy).

3.3. Importance of Severity, Extent, and Local Interannual Change in Air Temperature for LST and GPP Responses

The random forest models used to determine the importance of S, E, and T_{air} to the postdisturbance response in LST and GPP were cross validated using a 60% testing subset of the data. R^2 values of the relationship between predicted and actual data were 0.39 for LST and 0.45 for GPP (Table 2).

Across both response variable models, both S and T_{air} were the most important continuous variables in determining disturbance impacts according to MSE importance (Table 2). Both models also underscored the importance of disturbance type and ecoregion on LST and GPP. E had relatively low importance in the random forest models. The models had somewhat low predictive power, likely because all potential predictor variables were not included in the model. While the residual sum of squares (RSS) importance values were not used to determine variable importance, they corroborate the results using MSE importance (Table 2).

3.4. Long-Term Patterns and Trends in Disturbance Response

3.4.1. Fire

LST and GPP showed a short time to stabilization across all ecoregions following fire. In general, LST rose quickly in the first year postdisturbance and then followed a slight decline over the next 1–4 years (Figures 4 and S1), although LST remained elevated from predisturbance LST and even rose gradually over

Table 2. Summary of Random Forest Models Used to Predict LST and GPP[a]

Response Variable	Predictor Variable	% Increase in MSE	Increase in RSS	RMSE	MBE	Model R^2	Testing *n*	Training *n*
LST	Severity	20.13	13.3×10^6	2.49	0	0.39	1465320	976855
	Change in air *T*	16.25	10.6×10^6					
	Extent	7.72	2.32×10^5					
	Disturbance Type	16.07	3.78×10^5					
	Ecoregion	15.45	2.03×10^5					
GPP	Severity	14.95	8.88×10^7	18.73	−0.03	0.45	1465320	976697
	Change in air *T*	17.77	7.26×10^7					
	Extent	10.42	2.36×10^7					
	Disturbance Type	11.12	3.30×10^7					
	Ecoregion	13.78	3.22×10^7					

[a]The model R^2 value is the correlation between values predicted by the model and the actual values in the 60% testing subset of the data. The "% increase in MSE" is the increase in MSE that would occur if that predictor variable were removed from the model. The "increase in RSS" is the increase in RSS that would occur if the values of that variable were permuted across all nodes in all trees.

the remainder of the years following the decline. This pattern was consistent across ecoregions, with slight variations in the timing of the decline and in the level to which LST declined postdisturbance. As predicted, the severity (% decline in EVI) of the disturbance had a strong influence on the LST increase postdisturbance. Surprisingly, severity did not have an effect on the duration of the postdisturbance difference in LST. Ecosystem LST values appeared to decline just as quickly following high-severity fires as lower severity fires, although they retained higher LST than lower severity fires. GPP decreased over the first 1–2 years following fire and then increased back to a stable level over the following 2–12 years (Figures 5 and S6), although GPP remained lower than predisturbance levels for higher severity fires. Most

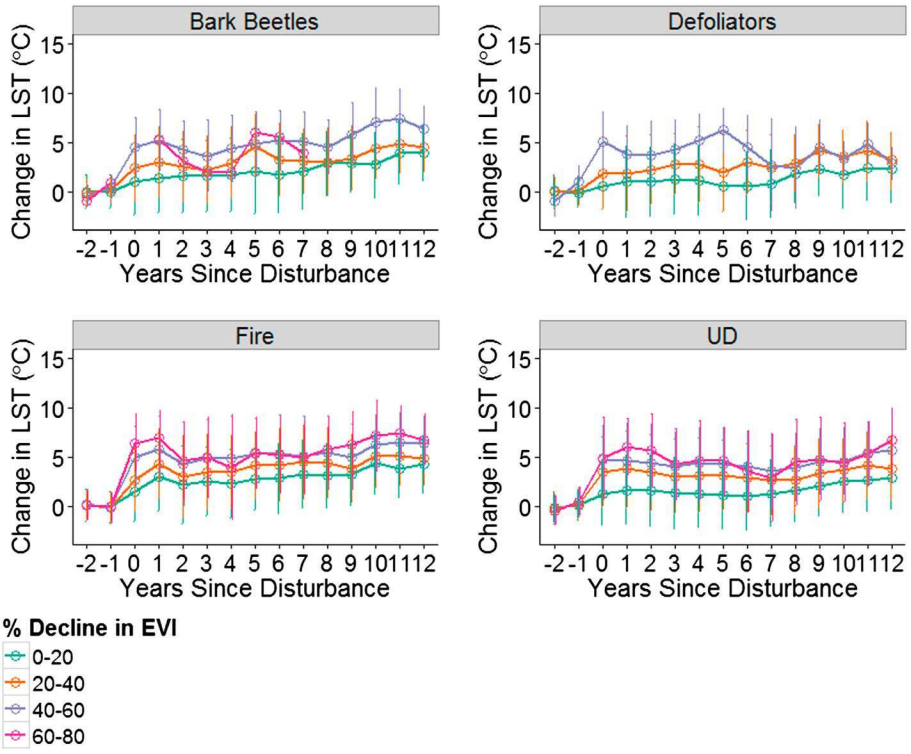

Figure 4. JJA change in LST (°C) following disturbance over the entire western U.S. See Figures S1–S4 for changes by ecoregion. In the case of bark beetles and defoliators, "year of disturbance" is defined as the year in which damage reaches a level detectable in the EVI time series.

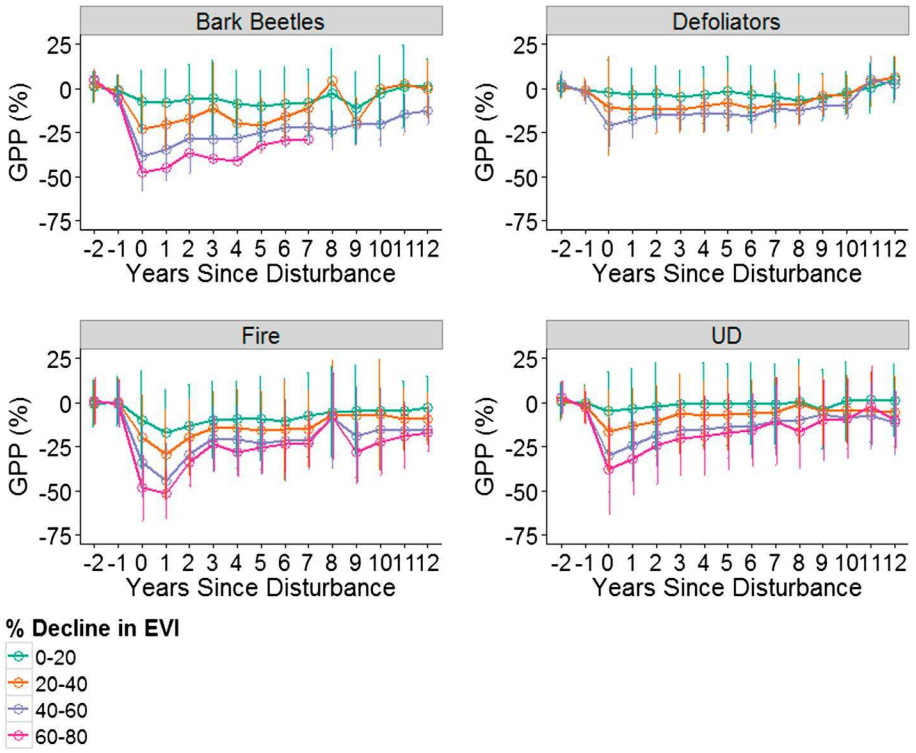

Figure 5. Percent JJA change in GPP following disturbance over the entire western U.S. See Figures S5–S8 for changes by ecoregion. In the case of bark beetles and defoliators, year of disturbance is defined as the year in which damage reaches a level detectable in the EVI time series.

regions showed a similar pattern, with varying degrees of differences between the severity categories. The highest-severity fires (> 60% decline in EVI) showed the largest declines in GPP. However, these fires did not show significantly different stabilization times than fires in other severity categories.

3.4.2. Bark Beetles

Generally, LST increased gradually in the 1–2 years following bark beetle disturbance and then stabilized at higher temperatures for the remainder of the postdisturbance years, with some recovery to slightly lower temperatures (Figures 4 and S2). This pattern was fairly consistent across ecoregions and severity levels, despite many of the ecoregions not having any bark beetle detections. In general, GPP declined in the year of the disturbance event and then recovered gradually over the next 3–12 years (Figures 5 and S7). Higher-severity attacks resulted in the sharpest declines and longest recovery times of GPP. Several regions did not show significant impacts of bark beetle disturbance on GPP.

3.4.3. Defoliators

The regions with data available for defoliator attacks showed an increase in LST in the 1–2 years after an attack (Figures 4 and S3), with higher-severity disturbances resulting in a larger increase in temperature. LST never fully recovered to predisturbance levels and actually increased over the period of observation, although the rate of increase slowed over time. In several regions and with lower severity disturbances, LST increased but did not decline over the period of available data. GPP declined in the year of disturbance in the Western Cordillera and Upper Gila Mountains ecoregions (Figures 5 and S8) and increased slightly in the Cold Desert and West/Central Semi-Arid Prairie ecoregions. GPP increased back to predisturbance levels over the remainder of the available time period in the two ecoregions that showed initial declines. In the ecoregions that showed GPP increases, GPP levels fluctuated around predisturbance levels.

3.4.4. Unidentified Disturbances

For the first 1–3 years following UDs, LST increased from predisturbance levels (Figures 4 and S4). LST showed slight indications of recovery (i.e., decreasing LST) in the 1–5 years following maximum LST increases but tended to stabilize at higher temperatures. Following UDs, GPP declined for 1–2 years (Figures 5 and S8) and then gradually increased for 1–9 years until stabilizing. In the Marine West Coast Forests it took a

much longer period of time for the very high-severity disturbances to recover compared to the other three disturbance categories.

3.4.5. Relationships Between Recovery and Initial Impacts

Recovery patterns following bark beetle, defoliator, and fire effects (Figures 4 and 5) are of similar magnitude and sign, seeming to contradict the results from section 3.1 (Figure 3). This is due to the separation of severity in the recovery figures. The severity categories do not contain equal numbers of pixels, and thus if the average is taken, bark beetle and defoliator LST and GPP responses are smaller than those following fire simply due to the inclusion of more low-severity disturbances. Additionally, as many of the pixels lie within the Western Cordillera ecoregion, the results of that ecoregion dominate the recovery results.

4. Discussion

4.1. Mechanisms Behind LST and GPP Responses to Disturbance

Our results indicate that LST increases and GPP decreases following forest disturbances in the western U.S., although these responses vary by ecoregion. These responses to tree mortality are expected, as mortality results in a loss of canopy photosynthesis and thus GPP. Previous research [e.g., *Bright et al*., 2013; *Maness et al*., 2013] has indicated that ET declines coincident with photosynthesis following disturbance. Decreases in ET result in shifts in the exchange of heat from latent to sensible heat, resulting in increased LST. Decreased albedo following fires also enhances absorption of radiation at the surface, further increasing LST. There are mixed results regarding the importance of albedo for impacting LST and radiative forcing following insect outbreaks or drought, with some results indicating little importance [*Bright et al*., 2013] and some indicating higher importance [*O'Halloran et al*., 2012]. Disturbance-related albedo changes may be more or less important to LST and radiative forcing at varying times of the year, with more importance in the winter due to snowpack effects (i.e., more exposed snow due to a loss of canopy cover) [*Randerson et al*., 2006; *O'Halloran et al*., 2012] and less importance in summer. Decreased surface shading by the canopy due to needle loss and/or snagfall and subsequent changes in soil moisture may also impact postdisturbance LST.

Despite showing a broad-scale reduction in GPP, some ecoregions showed an increase in GPP. This may occur through several mechanisms: (1) false classification of a pixel as disturbance due to natural fluctuations in the EVI signal, (2) predisturbance limitation of GPP by climate conditions, (3) release of the remaining vegetation from resource (light, nutrient, and/or water) limitation, or (4) an increase in the length of the growing season. The first and second mechanisms are the most probable in the case of UDs where detections may reflect random or phenological fluctuations in canopy greenness or temporary climate-induced declines in photosynthesis (e.g., due to drought). Natural fluctuations in the EVI signal may have been labeled as disturbance in some instances, resulting in false positives. Removal of climate limitations postdetection would allow "disturbance" pixels to increase in GPP, also resulting in false positives because no actual mortality occurred. The third mechanism is that partial canopy mortality, as may occur in insect outbreaks, may release any remaining vegetation from resource limitation, enhancing the productivity of the remaining vegetation enough to compensate for the partial or complete loss of the canopy, increasing GPP. Several studies [*Veblen et al*., 1991; *Brown et al*., 2012; *Reed et al*., 2014; *Pec et al*., 2015] have cited this mechanism to explain potential increases in productivity following insect disturbance. While the relatively low resolution of MODIS GPP is unlikely to detect small changes in GPP due to this mechanism, if the affected area is large enough, it may be sufficient. Finally, sites with increased GPP typically also had increased LST. As minimum temperature is a variable in the current GPP algorithm, slight increases in LST could extend the growing season and thus increase GPP.

4.2. Causes and Implications of Differences in Response Among Disturbance Types and Ecoregions

There were differences in LST and GPP responses to disturbance both between disturbance categories and ecoregions, although the general response patterns matched those from previous studies [e.g., *Coops and Wulder*, 2010; *Bright et al*., 2013; *Maness et al*., 2013; *Moore et al*., 2013]. We hypothesize that insect disturbances and UDs resulted in less severe responses than fires due to both the detection method used and the nature of the disturbances. Our disturbance detection algorithm may have recorded some pixels as disturbed that were experiencing decreased greenness that did not cause significant mortality, diminishing the category's overall disturbance response results. Additionally, bark beetle outbreaks, defoliator attacks, and

UDs tend to be somewhat species specific and may occur over several years [*Raffa et al*., 2008; *Bentz et al*., 2010]. Thus, small patches within larger pixels might be at differing successional stages at the time of observation [e.g., *Penn et al*., 2016]. These disturbance characteristics could decrease the disturbance LST and GPP response because few trees may be affected in a given area annually. This also could result in the inclusion of some mortality in our predisturbance LST and GPP response estimates. However, our recovery figures (Figures 4 and 5) indicate that the largest changes in magnitude of the variables occurred in the year of the detection. This suggests that most of the mortality or decrease in productivity occurred in the year of detection and not in previous years. Thus, we believe that the muting effect of gradual disturbances is very slight.

The variation in disturbance response among ecoregions is likely a result of regional variation in climate, forest composition and structure, soils, and hydrology, as well as disturbance regime. For example, postfire increases in LST were much lower in ecoregions with high precipitation and moderate temperatures (e.g., Marine West Coast Forests) than in ecoregions with low precipitation and higher temperatures (e.g., Upper Gila Mountains), likely due to greater water availability for latent heat exchange and lower atmospheric demand. Differences between ecoregions in terms of cloudiness may also account for some of the differences in disturbance responses. However, all response variables were preprocessed to minimize cloud cover and were JJA averages, when clouds are the least prevalent. The exact influence of environmental variables other than air temperature was not investigated in this study and merits further research.

The observed differences in disturbance response between ecoregions reinforce the importance of management strategies that are dependent on the disturbance locale. Current and predicted future climate [*PRISM Climate Group*, 2011; *Dobrowski et al*., 2013] and disturbance regimes [*Fulé et al*., 1997; *Franklin et al*., 2002] differ substantially between ecoregions. We show that response regimes (i.e., response magnitude, direction, and duration) also differ significantly. Variation in management strategies among ecoregions and other management divisions will have increasing importance as these components (i.e., climate, disturbance regime, and response regime) of climate disturbance feedbacks interact. This is especially true in areas where high-severity disturbance events may be increasing in frequency, as recovery to predisturbance biophysical characteristics may not occur, indicating longer-term shifts in ecosystem type or function. Managers should be wary of applying strategies aimed at mitigating disturbance-climate feedbacks from one region to another without validation.

4.3. Potential Disturbance Feedbacks to Local and Regional Climate

Disturbance severity (*S)* is critical to LST and GPP responses, as has been noted in many previous studies [*Randerson et al*., 2006; *Bond-Lamberty et al*., 2007; *Kurz et al*., 2008; *Maness et al*., 2013]. Disturbances are projected to increase in severity due to climate change [*Adams et al*., 2009; *Littell et al*., 2009; *Bentz et al*., 2010; *Westerling et al*., 2011; *Seidl et al*., 2014], indicating the presence of a positive feedback loop whereby changes in climate may result in more frequent and more severe disturbances, which then may result in greater LST and GPP feedbacks to climate. As severity was also linked to differences in postdisturbance recovery, longer feedbacks from disturbance to local climates may result as severity increases due to climate change. Longer disturbance impacts may lead to shifts in ecosystem type, as prolonged changes in the energy budgets of the area prevent the vegetation from fully recovering [e.g., *Breshears et al*., 2009; *Allen et al*., 2010]. However, the impacts of changes in disturbance regime on recovery patterns may be mitigated somewhat by a CO_2 fertilization effect, which potentially allows vegetation to grow more quickly due to enhanced photosynthetic efficiency [*Foster et al*., 2010; *McMahon et al*., 2010; *Williams et al*., 2012].

Years with warmer air temperatures also resulted in larger LST and GPP responses. As such, disturbance impacts are likely to be enhanced in areas where climate change will result in warmer conditions. Forest function may change more in response to future disturbances than it did in response to historic disturbances with the same severity and extent.

4.4. Scale and Its Role in Disturbance-Induced Climate Forcing

The variation in disturbance responses between disturbance types highlights the importance of scale in disturbance studies. Previous studies [e.g., *Kurz et al*., 2008; *Hicke et al*., 2013] found that insect outbreaks can result in potential impacts at least as large as fire. We did not see this in our results. However, nonfire disturbances are typically more spatially and temporally patchy than fires. Less continuous spatial patterns mean

that when aggregated across large pixels (e.g., 250 m), the disturbances appear to have a smaller effect. The use of 1 km GPP data may have exaggerated this effect. *Penn et al*. [2016] found that despite the large impacts on ET observed at the hillslope scale following a bark beetle outbreak, only small effects were seen at the watershed scale due to the mediating contribution of nearby healthy vegetation.

4.5. Disturbance Detection

The detection of low-severity disturbances and in particular insect-induced damage and mortality remains a challenge for remote sensing, particularly in cloud-dominated and mountainous regions. Evaluation efforts are further hampered by the limited availability of broad-scale repeated ground survey data. The BFAST/Hansen and VCT remotely sensed data sets we evaluated agreed well with each other and with MTBS polygons (Table S3). However, both data sets showed poor agreement with ADS maps (Table S3). This is not surprising, as ADS maps, while very useful at coarse resolutions for research or for forest planning purposes, have only low to moderate accuracy when compared to field plots [*Johnson and Ross*, 2008]. While ADS data are increasingly used in research studies on the extent and impacts of insect disturbance, these data have their own issues. For example, different observers conduct the surveys each year, and the methods used vary from region to region. More specifically, one observer might draw a small polygon around only a few trees, while another might draw a very large polygon around the same small area. ADS maps are subjective and represent general areas of disturbance, not precise disturbance locations [*Hall et al*., 2006; *Johnson and Ross*, 2008; *Johnson and Wittwer*, 2008]. Despite low agreement between our detection product and ADS, we believe that our combined approach, whereby we limit our ecosystem response results to areas where ADS also detected insect damage, is justified and preferable to using ADS alone to represent nonfire disturbances. The approach uses remotely detected data as a complement to ADS and MTBS data to more finely resolve the temporal and spatial variation in disturbance locations. Several studies have used this combined approach [*Hall et al*., 2006; *Assal et al*., 2014], in which aerial surveys bound an area, but remote sensing algorithms are used to discover the exact locations and timing of disturbances within those bounds. It is highly unlikely that detected disturbances within an aerial polygon represent a disturbance other than that marked by the survey. Although our disturbance detection is not perfectly accurate, it is statistically comparable to the results from the similar VCT remote sensing approach (Tables S3 and S4 and Figure S9). By limiting our data extent to areas of known disturbance, we can be confident that the detected points are indeed disturbance.

4.6. Assumptions and Errors

Several assumptions may have contributed to increased uncertainty in the results. While the BFAST method has proven effective at detecting disturbances such as fires, floods, and deforestation [*Verbesselt et al*., 2010a; *Watts and Laffan*, 2014; *DeVries et al*., 2015], the method's success may vary depending on local vegetation and disturbance type [*Watts and Laffan*, 2014]. We demonstrated that BFAST and Hansen data combined are able to detect the majority of large, moderate to severe, disturbances (Figures S9 and S10 and Tables S3 and S4). However, small or patchy disturbances may be missed at this resolution (250 m), leading to conservative results that are likely to be underestimates rather than overestimates of the total impacts of disturbance on forest ecosystems.

We may have also introduced some error by using all MTBS and ADS polygons, regardless of the severity reported in those polygons. However, our detection methods were designed to represent more spatially and temporally explicit disturbance locations and tended to pick up higher-severity disturbances than would have been found in a random subset of the disturbance polygons (Table S3). It is therefore unlikely that we include many nondisturbance pixels in low-severity polygons.

We also assume that the detected decline in EVI represents mortality, not simply a decline in canopy "greenness" related to temporary stressors such as high vapor pressure deficit. It is likely that these false positives are few [*Watts and Laffan*, 2014; *Dutrieux et al*., 2015] and occur primarily in the UD category. The use of fire, bark beetle, and defoliator polygons decreased the likelihood of false positives in those categories. Detected declines in EVI that did not represent mortality should result in a decrease in the magnitude of the response results, as nonmortality detections will decrease the average change observed. Additionally, we demonstrate the validity of EVI-based severity in Figure S10.

Issues of scale, especially pertaining to our use of 1 km GPP, may have also resulted in increased uncertainty. However, several other studies have investigated the effects of MPB on GPP and found reductions in GPP that overlap the 10–90% quantiles of our results (−27–21%). Results in the upper and lower quantiles of our data are not considered due to outliers. *Bright et al*. [2013], *Coops and Wulder* [2010], and *Moore et al*. [2013] found GPP declines of 5–26%, 15–20%, and 13–30%, respectively. *Coops and Wulder* [2010] studied MPB disturbance in British Columbia, and *Bright et al*. [2013] and *Moore et al*. [2013] studied MPB disturbance in Colorado. Both regions have experienced severe MPB damage. While our results overlapped zero and used the same MODIS GPP product to estimate changes in the variable, we also used coarser-resolution data to locate areas of likely disturbance (i.e., 240 m versus 30 m or field data) and included less severely disturbed areas in addition to severely disturbed areas.

Finally, the calculation of extent (*E*) may have contributed toward its insignificant relationship with disturbance responses. *E* was determined as the area of adjoining pixels that were affected by the same disturbance type. This method is slightly problematic as it assumes that bark beetle and defoliator disturbances in the same area represent the same outbreak. However, it is logical that *E* is less important than severity and interannual changes in air temperature for determining disturbance effects on LST and GPP.

5. Conclusions

We used satellite data to objectively determine the effects of four categories of disturbance on LST and GPP across nine ecoregions in the western U.S. We found that all disturbance types resulted in overall increased LST in the 2 years following disturbance, and all disturbance types but UD resulted in decreased GPP, although the exact magnitude and direction of these changes varied significantly both among disturbance types and ecoregions. Fires showed the largest and clearest impacts in all response variables, whereas bark beetle, defoliator, and UD responses were much less pronounced. Severity and interannual changes in air temperature were the primary drivers of the magnitude of disturbance response regardless of the type or location, and disturbances of higher severity resulted in longer recovery times. The results of this study suggest a strong potential climate feedback due to biophysical changes in forests following disturbance events that may strengthen as disturbances grow in frequency and severity in the coming decades. Despite several assumptions made in the study, to our knowledge this analysis remains the first to incorporate multiple disturbance types over a large geographical region in an evaluation of the effects of disturbance on ecosystem climate services. Future research utilizing both field and satellite observations in conjunction with ecosystem simulations is required to advance our understanding of ecosystem responses to interactions between climate and disturbance.

Acknowledgments

We thank T. Fletcher, C. Reed, Z. Liu, S. Smith, and the participants of the Department of Ecosystem and Conservation Science fall 2015 seminar for comments on the analysis and manuscript. This research was supported through a USDA McIntyre-Stennis Grant to A.B. and NASA Earth and Space Science Fellowship NNX15AN16H to L.A.C. E.L. was supported by Forest Service agreements 11-JV-11221637-186 and 10-CA-11010000-026. Z.H., E.L., and L.A.C. were supported through a NASA Applied Wildland Fire Applications award (agreement NNH11ZDA001N-FIRES). Summaries of the data used in this study are found in the supporting information. Full data sets and code used in this study are available by contacting Annie Cooper (leila.cooper@umontana.edu). L.A. Cooper and A. Ballantyne designed the study. L.A. Cooper carried out the study, with assistance from A. Ballantyne, Z. Holden, and E. Landguth. L.A. Cooper wrote the manuscript with contributions from all authors.

References

Adams, H. D., M. Guardiola-Claramonte, G. A. Barron-Gafford, J. C. Villegas, D. D. Breshears, C. B. Zou, P. A. Troch, and T. E. Huxman (2009), Temperature sensitivity of drought-induced tree mortality portends increased regional die-off under global-change-type drought, *Proc. Natl. Acad. Sci. U.S.A.*, *106*(17), 7063–7066, doi:10.1073/pnas.0901438106.

Allen, C. D., et al. (2010), A global overview of drought and heat-induced tree mortality reveals emerging climate change risks for forests, *For. Ecol. Manag.*, *259*(4), 660–684, doi:10.1016/j.foreco.2009.09.001.

Anderegg, W. R. L., J. M. Kane, and L. D. L. Anderegg (2013), Consequences of widespread tree mortality triggered by drought and temperature stress, *Nat. Clim. Chang.*, *3*(1), 30–36, doi:10.1038/nclimate1635.

Assal, T. J., J. Sibold, and R. Reich (2014), Modeling a historical mountain pine beetle outbreak using Landsat MSS and multiple lines of evidence, *RemoteSens. Environ.*, *155*, 275–288, doi:10.1016/j.rse.2014.09.002.

Bentz, B. J., J. Régnière, C. J. Fettig, E. M. Hansen, J. L. Hayes, J. A. Hicke, R. G. Kelsey, J. F. Negrón, and S. J. Seybold (2010), Climate change and bark beetles of the western United States and Canada: Direct and indirect effects, *Bioscience*, *60*(8), 602–613, doi:10.1525/bio.2010.60.8.6.

Bonan, G. B. (2008), Forests and climate change: Forcings, feedbacks, and the climate benefits of forests, *Science*, *320*(5882), 1444–1449, doi:10.1126/science.1155121.

Bond-Lamberty, B., S. D. Peckham, D. E. Ahl, and S. T. Gower (2007), Fire as the dominant driver of central Canadian boreal forest carbon balance, *Nature*, *450*(7166), 89–92, doi:10.1038/nature06272.

Breshears, D. D., O. B. Myers, C. W. Meyer, F. J. Barnes, C. B. Zou, C. D. Allen, N. G. McDowell, and W. T. Pockman (2009), Tree die-off in response to global change-type drought: Mortality insights from a decade of plant water potential measurements, *Front. Ecol. Environ.*, *7*(4), 185–189, doi:10.1890/080016.

Bright, B. C., J. A. Hicke, and A. J. H. Meddens (2013), Effects of bark beetle-caused tree mortality on biogeochemical and biogeophysical MODIS products, *J. Geophys. Res. Biogeosci.*, *118*, 974–982, doi:10.1002/jgrg.20078.

Brown, M. G., et al. (2012), The carbon balance of two lodgepole pine stands recovering from mountain pine beetle attack in British Columbia, *Agric. Forest Meteorol.*, *153*, 82–93, doi:10.1016/j.agrformet.2011.07.010.

Coops, N. C., and M. A. Wulder (2010), Estimating the reduction in gross primary production due to mountain pine beetle infestation using satellite observations, *Int. J. Remote Sens.*, *31*(8), 2129–2138, doi:10.1080/01431160903474947.

DiMiceli, C. M., M. L. Carroll, R. A. Sohlberg, C. Huang, M. C. Hansen, and J. R. G. Townshend (2011), *Annual Global Automated MODIS Vegetation Continuous Fields (MOD44B) at 250 m Spatial Resolution for Data Years Beginning Day 65, 2000–2010, Collection 5 Percent Tree Cover*, Univ. of Maryland, College Park, Md. [Available at http://glcf.umd.edu/data/vcf/.]

DeVries, B., J. Verbesselt, L. Kooistra, and M. Herold (2015), Robust monitoring of small-scale forest disturbances in a tropical montane forest using Landsat time series, *Remote Sens. Environ.*, *161*, 107–121, doi:10.1016/j.rse.2015.02.012.

Dillon, G. K., Z. A. Holden, P. Morgan, M. A. Crimmins, E. K. Heyerdahl, and C. H. Luce (2011), Both topography and climate affected forest and woodland burn severity in two regions of the western US, 1984 to 2006, *Ecosphere*, *2*(12), 1–33, doi:10.1890/ES11-00271.1.

Dobrowski, S. Z., J. Abatzoglou, A. K. Swanson, J. A. Greenberg, A. R. Mynsberge, Z. A. Holden, and M. K. Schwartz (2013), The climate velocity of the contiguous United States during the 20th century, *Glob. Chang. Biol.*, *19*(1), 241–251, doi:10.1111/gcb.12026.

Dutrieux, L. P., J. Verbesselt, L. Kooistra, and M. Herold (2015), Monitoring forest cover loss using multiple data streams: A case study of a tropical dry forest in Bolivia, *ISPRS J. Photogramm. Remote Sens.*, *107*, 112–125, doi:10.1016/j.isprsjprs.2015.03.015.

Eidenshink, J., B. Schwind, K. Brewer, Z.-L. Zhu, B. Quayle, and S. Howard (2007), A project for monitoring trends in burn severity, *Fire Ecol.*, *3*(1), 3–21, doi:10.4996/fireecology.0301003.

Esri (2010), *ArcGIS Desktop: Release 10*, *Environmental Systems Research Institute*, Redlands, Calif.

Foster, J. R., J. l. Burton, J. A. Forrester, F. Liu, J. D. Muss, F. M. Sabatini, R. M. Scheller, and D. J. Mladenoff (2010), Evidence for a recent increase in forest growth is questionable, *Proc. Natl. Acad. Sci. U.S.A.*, *107*(21), E86–E87, doi:10.1073/pnas.1002725107.

Franklin, J. F., et al. (2002), Disturbances and structural development of natural forest ecosystems with silvicultural implications, using Douglas-fir forests as an example, *For. Ecol. Manag.*, *155*(1–3), 399–423, doi:10.1016/S0378-1127(01)00575-8.

Fulé, P. Z., W. W. Covington, and M. M. Moore (1997), Determining reference conditions for ecosystem management of southwestern ponderosa pine forests, *Ecol. Appl.*, *7*(3), 895–908, doi:10.1890/1051-0761(1997)007[0895:DRCFEM]2.0.CO;2.

Hall, R. J., R. S. Skakun, and E. J. Arsenault (2006), Remotely sensed data in the mapping of insect defoliation, in *Understanding Forest Disturbance and Spatial Pattern: Remote Sensing and GIS Approaches*, edited by M. A. Wulder and S. E. Franklin, pp. 85–111, Taylor and Francis, CRC Press, Boca Raton, Fla.

Hansen, M. C., et al. (2013), High-resolution global maps of 21st-century forest cover change, *Science*, *342*(6160), 850–853, doi:10.1126/science.1244693.

Hanson, P. J., and J. F. Weltzin (2000), Drought disturbance from climate change: Response of United States forests, *Sci. Total Environ.*, *262*(3), 205–220, doi:10.1016/S0048-9697(00)00523-4.

Heyder, U., S. Schaphoff, D. Gerten, and W. Lucht (2011), Risk of severe climate change impact on the terrestrial biosphere, *Environ. Res. Lett.*, *6*(3), 034–036, doi:10.1088/1748-9326/6/3/034036.

Hicke, J. A., et al. (2012), Effects of biotic disturbances on forest carbon cycling in the United States and Canada, *Glob. Chang. Biol.*, *18*(1), 7–34, doi:10.1111/j.1365-2486.2011.02543.x.

Hicke, J. A., A. J. H. Meddens, C. D. Allen, and C. A. Kolden (2013), Carbon stocks of trees killed by bark beetles and wildfire in the western United States, *Environ. Res. Lett.*, *8*, 035032, doi:10.1088/1748-9326/8/3/035032.

Holden, Z. A., P. Morgan, and J. S. Evans (2009), A predictive model of burn severity based on 20 year satellite-inferred burn severity data in a large southwestern US wilderness area, *For. Ecol. Manag.*, *258*(11), 2399–2406, doi:10.1016/j.foreco.2009.08.017.

Huang, C., S. N. Goward, J. G. Masek, N. Thomas, Z. Zhu, and J. E. Vogelmann (2010), An automated approach for reconstructing recent forest disturbance history using dense Landsat time series stacks, *Remote Sens. Environ.*, *114*(1), 183–198, doi:10.1016/j.rse.2009.08.017.

Huete, A., K. Didan, T. Miura, E. P. Rodriguez, X. Gao, and L. G. Ferreira (2002), Overview of the radiometric and biophysical performance of the MODIS vegetation indices, *Remote Sens. Environ.*, *83*(1–2), 195–213, doi:10.1016/S0034-4257(02)00096-2.

Jassby A. D., and J. E. Cloern (2015), Wq: Some tools for exploring water quality monitoring data, R package version 0.4.3. [Available at https://cran.r-project.org/package=wq.]

Johnson, E. A., K. Miyanishi, and J. M. H. Weir (1998), Wildfires in the western Canadian boreal forest: Landscape patterns and ecosystem management, *J. Veg. Sci.*, *9*(4), 603–610, doi:10.2307/3237276.

Johnson, E. W., and J. Ross (2008), Quantifying error in aerial survey data, *Aust. For.*, *71*(3), 216–222, doi:10.1080/00049158.2008.10675038.

Johnson, E. W., and D. Wittwer (2008), Aerial detection surveys in the United States, *Aust. For.*, *71*(3), 212–215, doi:10.1080/00049158.2008.10675037.

Kurz, W. A., C. C. Dymond, G. Stinson, G. J. Rampley, E. T. Neilson, A. L. Carroll, T. Ebata, and L. Safranyik (2008), Mountain pine beetle and forest carbon feedback to climate change, *Nature*, *452*(7190), 987–990, doi:10.1038/nature06777.

Law, B. E., O. J. Sun, J. Campbell, S. Van Tuyl, and P. E. Thornton (2003), Changes in carbon storage and fluxes in a chronosequence of ponderosa pine, *Glob. Chang. Biol.*, *9*(4), 510–524, doi:10.1046/j.1365-2486.2003.00624.x.

Liaw, A., and M. Wiener (2002), Classification and regression by randomForest, *R News*, *2*(3), 18–22.

Littell, J. S., D. McKenzie, D. L. Peterson, and A. L. Westerling (2009), Climate and wildfire area burned in western U.S. ecoprovinces, 1916–2003, *Ecol. Appl.*, *19*(4), 1003–1021, doi:10.1890/07-1183.1.

Liu, H. Q., and A. R. Huete (1995), A feedback based modification of the NDVI to minimize canopy background and atmospheric noise, *IEEE Trans. Geosci. Remote Sens.*, *33*(2), 457–465, doi:10.1109/36.377946.

Maness, H., P. J. Kushner, and I. Fung (2013), Summertime climate response to mountain pine beetle disturbance in British Columbia, *Nat. Geosci.*, *6*(1), 65–70, doi:10.1038/ngeo1642.

McMahon, S. M., G. G. Parker, and D. F. Miller (2010), Evidence for a recent increase in forest growth, *Proc. Natl. Acad. Sci. U.S.A.*, *107*(8), 3611–3615, doi:10.1073/pnas.0912376107.

Meddens, A. J. H., J. A. Hicke, and C. A. Ferguson (2012), Spatiotemporal patterns of observed bark beetle-caused tree mortality in British Columbia and the western United States, *Ecol. Appl.*, *22*(7), 1876–1891, doi:10.1890/11-1785.1.

Millar, C. I., and N. L. Stephenson (2015), Temperate forest health in an era of emerging megadisturbance, *Science*, *349*(6250), 823–826, doi:10.1126/science.aaa9933.

Moore, D. J. P., N. A. Trahan, P. Wilkes, T. Quaife, B. B. Stephens, K. Elder, A. R. Desai, J. Negron, and R. K. Monson (2013), Persistent reduced ecosystem respiration after insect disturbance in high elevation forests, *Ecol. Lett.*, *16*(6), 731–737, doi:10.1111/ele.12097.

O'Halloran, T. L., et al. (2012), Radiative forcing of natural forest disturbances, *Glob. Chang. Biol.*, *18*(2), 555–565, doi:10.1111/j.1365-2486.2011.02577.x.

Omernik, J. M. (1987), Ecoregions of the conterminous United States, *Annals of the Asso. Am. Geograph.*, *77*(1), 118–125, doi:10.1111/j.1467-8306.1987.tb00149.x.

Omernik, J. M., and G. E. Griffith (2014), Ecoregions of the conterminous United States: Evolution of a hierarchical spatial framework, *Environ. Manage.*, *54*(6), 1249–1266, doi:10.1007/s00267-0140364-1.

Pec, G. J., J. Karst, A. N. Sywenky, P. W. Cigan, N. Erbilgin, S. W. Simard, and J. F. Cahill (2015), Rapid increases in forest understory diversity and productivity following a mountain pine beetle (*Dendroctonus ponderosae*) outbreak in pine forests, *PLoS One*, *10*(4), e0124691, doi:10.1371/journal.pone.0124691.

Penn, C. A., L. A. Bearup, R. M. Maxwell, and D. W. Clow (2016), Numerical experiments to explain multiscale hydrological responses to mountain pine beetle tree mortality in a headwater watershed, *Water Resour. Res.*, *52*, 3143–3161, doi:10.1002/2015WR018300.

Pregitzer, K. S., and E. S. Euskirchen (2004), Carbon cycling and storage in world forests: Biome patterns related to forest age, *Glob. Chang. Biol.*, *10*(12), 2052–2077, doi:10.1111/j.13652486.2004.00866.x.

PRISM Climate Group (2011), *PRISM Climate Data*, Oregon State Univ., Corvallis, Ore. [Available at http://prism.oregonstate.edu.]

R Core Team (2013), *R: A Language and Environment for Statistical Computing*, *R Foundation for Statistical Computing*, Vienna, Austria. [Available at http://www.R-project.org/.]

Raffa, K. F., B. H. Aukema, B. J. Bentz, A. L. Carroll, J. A. Hicke, M. G. Turner, and W. H. Romme (2008), Cross-scale drivers of natural disturbances prone to anthropogenic amplification: The dynamics of bark beetle eruptions, *Bioscience*, *58*(6), 501, doi:10.1641/B580607.

Randerson, J. T., et al. (2006), The impact of boreal forest fire on climate warming, *Science*, *314*(5802), 1130–1132, doi:10.1126/science.1132075.

Reed, D. E., B. E. Ewers, and E. Pendall (2014), Impact of mountain pine beetle induced mortality on forest carbon and water fluxes, *Environ. Res. Lett.*, *9*(10), 105004, doi:10.1088/17489326/9/10/105004.

Seidl, R., M. J. Schelhaas, W. Rammer, and P. J. Verkerk (2014), Increasing forest disturbances in Europe and their impact on carbon storage, *Nat. Clim. Change*, *4*, 806–810, doi:10.1038/nclimate2318.

Sobrino, J. A., J. C. Jimenez-Munoz, and L. Paolini (2004), Land surface temperature retrieval from LANDSAT TM 5, *Remote Sens. Environ.*, *90*(4), 434–440, doi:10.1016/j.rse.2004.02.003.

Sousa, W. P. (1984), The role of disturbance in natural communities, *Annu. Rev. Ecol. Syst.*, *15*, 353–391, doi:10.1146/annurev.es.15.110184.002033.

Townshend, J., M. Hansen, M. Carroll, C. DiMiceli, R. Sohlberg, and C. Huang (2011), User guide for the MODIS vegetation continuous fields product Collection 5 version 1, Univ. of Maryland. [Available at http://glcf.umd.edu/library/guide/VCF_C5_UserGuide_Dec2011.pdf.]

Vanderhoof, M., C. A. Williams, B. Ghimire, and J. Rogan (2013), Impact of mountain pine beetle outbreaks on forest albedo and radiative forcing, as derived from Moderate Resolution Imaging Spectroradiometer, Rocky Mountains, USA, *J. Geophys. Res. Biogeosci.*, *118*, 1461–1471, doi:10.1002/jgrg.20120.

Veblen, T. T., K. S. Hadley, M. S. Reid, and A. J. Rebertus (1991), The response of subalpine forests to spruce beetle outbreak in Colorado, *Ecology*, *72*(1), 213–231, doi:10.2307/1938916.

Venables, W. N., and B. D. Ripley (2002), *Modern Applied Statistics With S*, 4th ed., Springer, New York.

Verbesselt, J., R. Hyndman, G. Newnham, and D. Culvenor (2010a), Detecting trend and seasonal changes in satellite image time series, *Remote Sens. Environ.*, *114*(1), 106–115, doi:10.1016/j.rse.2009.08.014.

Verbesselt, J., R. Hyndman, A. Zeileis, and D. Culvenor (2010b), Phenological change detection while accounting for abrupt and gradual trends in satellite image time series, *Remote Sens. Environ.*, *114*(12), 2970–2980, doi:10.1016/j.rse.2010.08.003.

Watson, R. T., M. C. Zinyowera, and R. H. Moss (1998), *The Regional Impacts of Climate Change: An Assessment of Vulnerability*, 22 pp., Cambridge Univ. Press, Cambridge.

Watts, L. M., and S. W. Laffan (2014), Effectiveness of the BFAST algorithm for detecting vegetation response patterns in a semi-arid region, *Remote Sens. Environ.*, *154*, 234–245, doi:10.1016/j.rse.2014.08.023.

Weng, Q., D. Lu, and J. Schubring (2004), Estimation of land surface temperature-vegetation abundance relationship for urban heat island studies, *Remote Sens. Environ.*, *89*(4), 467–483, doi:10.1016/j.rse.2003.11.005.

Westerling, A. L., M. G. Turner, E. A. H. Smithwick, W. H. Romme, and M. G. Ryan (2011), Continued warming could transform Greater Yellowstone fire regimes by mid-21st century, *Proc. Natl. Acad. Sci. U.S.A.*, *108*(32), 13,165–131,70, doi:10.1073/pnas.1110199108.

Williams, C. A., G. J. Collatz, J. Masek, and S. N. Goward (2012), Carbon consequences of forest disturbance and recovery across the conterminous United States, *Global Biogeochem. Cycles*, *26*, GB1005, doi:10.1029/2010GB003947.

Zhao, F., C. Huang, and Z. Zhu (2015), Use of vegetation change tracker and support vector machine to map disturbance types in Greater Yellowstone Ecosystems in a 1984–2010 Landsat time series, *IEEE Geosci. Rem. Sens. Lett.*, *12*(8), 1650–1654, doi:10.1109/LGRS.2015.2418159.